Video Article

Characterization of Nanocrystal Size Distribution using Raman Spectroscopy with a Multi-particle Phonon Confinement Model

İlker Doğan[1], Mauritius C. M. van de Sanden[1,2]

[1]Department of Applied Physics, Eindhoven University of Technology

[2]Dutch Institute for Fundamental Energy Research

Correspondence to: İlker Doğan at i.dogan@tue.nl

Abstract

Analysis of the size distribution of nanocrystals is a critical requirement for the processing and optimization of their size-dependent properties. The common techniques used for the size analysis are transmission electron microscopy (TEM), X-ray diffraction (XRD) and photoluminescence spectroscopy (PL). These techniques, however, are not suitable for analyzing the nanocrystal size distribution in a fast, non-destructive and a reliable manner at the same time. Our aim in this work is to demonstrate that size distribution of semiconductor nanocrystals that are subject to size-dependent phonon confinement effects, can be quantitatively estimated in a non-destructive, fast and reliable manner using Raman spectroscopy. Moreover, mixed size distributions can be separately probed, and their respective volumetric ratios can be estimated using this technique. In order to analyze the size distribution, we have formulized an analytical expression of one-particle PCM and projected it onto a generic distribution function that will represent the size distribution of analyzed nanocrystal. As a model experiment, we have analyzed the size distribution of free-standing silicon nanocrystals (Si-NCs) with multi-modal size distributions. The estimated size distributions are in excellent agreement with TEM and PL results, revealing the reliability of our model.

Video Link

The video component of this article can be found at http://www.jove.com/video/53026/

Introduction

Semiconductor nanocrystals draw attention as their electronic and optical properties can be tuned by simply changing their size in the range compared to their respective exciton-Bohr radii.[1] These unique size-dependent features make these nanocrystals relevant for various technological applications. For instance, carrier multiplication effects, observed when a high energy photon is absorbed by the nanocrystals of CdSe, Si, and Ge, can be used in the concept of spectrum conversion in solar cell applications;[2-4] or size-dependent optical emission from PbS-NCs and Si-NCs can be used in the light emitting diode (LED) applications.[5,6] A precise knowledge and control on the nanocrystal size distribution will therefore play a determinant role on the reliability and the performance of these technological applications based on nanocrystals.

The commonly used techniques for the size distribution and morphology analysis of nanocrystals can be listed as X-ray diffraction (XRD), transmission electron microscopy (TEM), photoluminescence spectroscopy (PL), and Raman spectroscopy. XRD is a crystallographic technique that reveals morphological information of the analyzed material. From the broadening of the diffraction peak, estimation of the nanocrystal size is possible,[7] however, obtaining a clear data is usually time consuming. Moreover, XRD can only enable the calculation of average of the nanocrystal size distribution. In the existence of multi-modal size distributions, size analysis with XRD can be misleading and result in wrong interpretations. TEM is a powerful technique that enables imaging of the nanocrystals.[8] Although TEM is able to reveal the presence of individual distributions in a multi-modal size distribution, sample preparation issue is always an effort to be spent before the measurements. In addition, working on densely packed nanocrystal ensembles with different sizes is challenging because of the difficulty of individual nanocrystal imaging. Photoluminescence spectroscopy (PL) is an optical analysis technique, and optically active nanocrystals can be diagnosed. Nanocrystal size distribution is obtained from the size-dependent emission.[9] Due to their poor optical properties of indirect band gap nanoparticles, large nanocrystals that are not subject to confinement effects, and defect-rich small nanocrystals cannot be detected by PL and the observed size distribution is only limited to nanocrystals with good optical properties. Although each of these abovementioned techniques has its own advantages, none of them have the capability of meeting the expectations (that is, being fast, non-destructive, and reliable) from and idealized size analysis technique.

Another means of size distribution analysis of nanocrystals is Raman spectroscopy. Raman spectroscopy is widely available in most of the labs, and it is a fast and non-destructive technique. In addition, in most cases, sample preparation is not required. Raman spectroscopy is a vibrational technique, which can be used to obtain information on different morphologies (crystalline or amorphous), and size-related information (from the size-dependent shift in the phonon modes that appear in the frequency spectrum) of the analyzed material.[10] The unique feature of Raman spectroscopy is that, while size-dependent changes are observed as a shift in the frequency spectrum, the shape of the phonon peak (broadening, asymmetry) gives information on the shape of the nanocrystal size distribution. Therefore it is in principle possible to extract the

necessary information, *i.e.*, the mean size and the shape factor, from Raman spectrum to obtain the size distribution of nanocrystals analyzed. In the case of multi-modal size distributions sub-distributions can also be separately identified via deconvolution of the experimental Raman spectrum.

In the literature, two theories are commonly referred to model the effect of nanocrystal size distribution on the shape of the Raman spectrum. The bond polarizability model (BPM)[11] describes the polarizability of a nanocrystal from the contributions of all the bonds within that size. The one-particle phonon confinement model (PCM)[10] uses size-dependent physical variables, *i.e.*, crystal momentum, phonon frequency and dispersion, and the degree of confinement, to define the Raman spectrum of a nanocrystal with a specific size. Since these physical variables depend on the size, an analytical representation of the PCM that can be explicitly formulized as a function of nanocrystal size can be defined. Projecting this expression on a generic size distribution function will therefore be able to account for the effect of size distribution within the PCM, which can be used to determine the nanocrystal size distribution from the experimental Raman spectrum.[12]

Protocol

1. Planning of the Experiments

1. Synthesize or obtain the nanocrystals of interest[13] (**Figure 1a**).
2. Avoid any confusion with the background signal by making sure that the substrate material does not have overlapping peaks in the Raman spectrum of the nanocrystals (**Figure 1a**).
3. Turn on the laser of the Raman spectroscopy setup. Wait enough time (approximately 15 min) for the laser intensity to stabilize.
4. Measure a bulk reference of the nanomaterial to be analyzed[12] (**Figure 1b**), following the measurement steps described in Step 2. From the peak position of the bulk material, estimate the relative shift[12].
5. Estimate the required laser power for Raman measurements using different powers on the nanocrystals going to be measured. Start a measurement with the lowest possible power to get enough signal (the ratio of the peak intensity to the background noise should be at least 50) , and increase the laser power if needed, as long as the position and shape of the nanocrystal Raman peak stays same[12,13].

2. Raman Spectroscopy of the Nanocrystal of Interest

1. Load the sample with nanocrystal powder deposited on the substrate into the measurement chamber.
   Note: The substrate dimensions are not critical (can be from millimeters to tens of centimeters) as long as it fits to the sample holder stage. The powder or thin film thickness should be at least tens of nanometers to have detectable signal from Raman spectroscope. For the planar substrate holder stage, simply lay the substrate under the optics (**Figure 1b**).
   1. Make sure the "Laser" and "Active" lights are off before opening the door in order to be safe from the unwanted illumination of the operating laser. If these lights are not off, perform the actions in steps 2.5 and 2.6. The "Interlock" sign always stays on.
   2. Press "Door Release" and open the door of the measurement chamber, and put the sample onto the sample holder stage (**Figure 1b**).
2. Adjust the focusing of the sample to be measured to get the highest possible signal.
   1. Select 50X objective and focus on the surface of the nanocrystal powder (**Figure 1b**).
   2. Bring the sample under focus using the z-direction manipulator of the sample holder. Check the clarity of the focused image from the live camera view on the computer screen.
   3. Close the door of the measurement chamber.
   4. Remove the shutter by clicking the "shutter-out" button from the Renishaw software, and let the laser light shine on the sample to be measured. Observe that the "Laser" and "Active" signs now flash green and blink red, respectively. In the live image from the screen, the laser will be visible (**Figure 1c**).
   5. From the live image, fine-tune the focusing of the sample using the wheel manipulator until the smallest laser spot, which is the best focus, is observed on the live image.
3. Set up a measurement from the Renishaw analysis software as described below (**Figure 1d**).
   1. From "Measurement" select new spectral acquisition option.
   2. From the pop-up window, set the measurement range from 150 to 700 cm^{-1}, set the time for the measurement as 30 sec, the total number of acquisition as 2x, and the percentage of the laser power as 0.5% (of a 25 mW laser) to be used during the measurement. Accept the parameters inserted, and the window will be closed.
   3. Start the measurement by clicking on the acquisition start button on the menu-bar. During the measurement the "Laser" and the "Active" lights will remain on.
4. Do not open the measurement chamber when these lights are on as the laser is in operation and measurement is being performed.
5. After the measurement is finished, put the shutter in by clicking the "shutter in" button from the Renishaw software. Observe that the lights of the "Laser" and the "Active" are turned off. Press "Door Release" and then open the door of the measurement chamber.
6. Before taking the sample out, lower the sample holder stage with the z-manipulator until there is a safe distance between the measured sample and the surface of the magnifying lens to remove the sample. Then, put the sample back to its container.
7. Turn off the laser.
8. Save the data in Renishaw software format, ".wxd", and in the text file format, ".txt". The latter will be used for the analysis of the experimental data.

3. Size Distribution Determination of the Nanocrystal of Interest

1. Open the text files of the measurements for the nanocrystal measurement, and the bulk reference.

2. Before plotting the data, smooth them using cubic spline, and normalize the data to 1 at their highest peak positions in order to have a good comparison of the relative peak shifts.
3. Plot the silicon nanocrystal and reference silicon data, determine the peak position of reference silicon, and estimate the amount of the shift, if any, from the actual peak position of 521 cm^{-1}.[12] Then save the processed silicon nanocrystal data as .txt file.
4. Start the fitting procedure.
    1. For the fitting procedure, type the fitting function shown at **Figure 2f** into an analysis program such as Mathematica.
    2. Import the normalized and corrected data as the input for the non-linear fitting model using the "Import" command.
    3. Ensure that the interval for skewness is between 0.1 and 1.0, and the mean size interval is between 2 nm and 20 nm.
    4. If necessary, insert additional peak(s) under the measured peak using the fitting function and repeat the steps 3.4.2 and 3.4.3 to fit the other sub-distribution(s).
    5. Press "Shift+Enter" to perform the fitting procedure.
    6. After that, insert the obtained values for the mean size and the skewness in the pre-defined generic distribution function shown at **Figure 2b**.
    7. After that, insert the obtained values for the mean size, D_0, and the skewness, σ, in the pre-defined generic distribution function shown in **Figure 2b**.
    8. Set the lower boundary of the of the integral as 1 nm. Set the upper limit of the integration to any size that does not exhibit any shift in the Raman spectrum (20 nm for Si-NCs)[12].
    9. Integrate the distribution function in **Figure 2b** as a function of nanocrystal size using the integral function definition a data analysis and plotting program by setting the lower and higher sizes as integral boundaries (1-20 nm for Si-NCs). Plot $\Phi(D)$ vs. D to give the size distribution. Alternatively, find a set of $\Phi(D)$ values for each value of D (for instance, from 1 to 20 nm for Si-NCs with an increment of 1 nm) and plot $\Phi(D)$ vs. D, which is the size distribution.
    10. If a multi-modal size distribution exists, first define the peaks to be fitted for other size distributions. Then, estimate their volume fractions of different size distributions with respect to each other by first finding the areas of each peaks obtained after deconvolution of the measurement data (with the size distribution determination procedure) and then calculating the areal ratio of each peak with respect to the total Raman peak.

Representative Results

For using Raman spectroscopy as a size analysis tool, a model to extract the size-related information from a measured Raman spectrum is needed. **Figure 2** summarizes the analytical multi-particle phonon confinement model.[12] All-size-dependent phonon confinement function (**Figure 2c**) is projected onto a generic size distribution function (**Figure 2b**), which is chosen as a lognormal distribution function. Given the amplitude (**Figure 2d**), full width at half maximum (**Figure 2e**), and the frequency shift (**Figure 2f**) value, this model can successfully be used to determine the size distribution.

Figure 3 envisages the use of multi-particle phonon confinement model to determine the size distribution of Si-NCs (details will follow). Si-NCs used in this analysis have a bimodal size distribution of small and large Si-NCs as shown in the TEM image.[13] According to TEM size analysis (not shown here), small Si-NCs have a distribution in the range 2-10 nm, and large Si-NCs have a distribution in the range 40-120 nm. The analysis of the Raman spectrum at the left panel reveals that the size distribution of small Si-NCs are indeed in the range 2-10 nm. The distribution is lognormal with a mean size of 4.2 nm, and with a skewness (shape anisotropy factor) of 0.27.

Figure 4 represents a detailed comparative analysis of Si-NCs synthesized using different precursor flows in the plasma enhanced chemical vapor deposition (PECVD) system. For fitting the as-measured Raman data, we used two fitting functions knowing that we had two sub-distributions in the Si-NC mixture. Since Si does not show size-dependent peak-shift for the sizes larger than 20 nm, a bulk-like Lorentzian peak can be assigned for large Si-NCs, which are in the range 40-120 nm in this case (represented as "Large Si-NCs" in the plot). For small Si-NCs, we used the multi-particle phonon confinement model as the fitting function (represented as "Small Si-NCs" in the plot). The mean size, and the skewness of the size distribution are obtained from this fit, which are the necessary parameters to plot the size distribution demonstrated in **Figure 2b**. This fitting function can be integrated up to the size from which a peak-shift is not observed any more, *i.e.*, 20 nm for Si-NCs. Results show that we can successfully determine the mean size, skewness, and the complete size distribution of Si-NCs (panel c and d) using Raman spectroscopy. Moreover, the volume fraction of small Si-NCs and large Si-NCs can be determined by the ratio of integrated peak areas. For Si-NCs synthesized using 3 sccs (standard cubic centimeters per second) of SiH_4 flow, the volume fraction of small Si-NCs was 80%, while for the case of 10 sccs SiH_4 flow, small Si-NC volume fraction is 88%.

Figure 5 demonstrates the comparison of determined average particle size of Si-NCs from various techniques. First, our analytical-PCM[12] (stars) is in very good agreement with the PCM.[10] Second, the results obtained from Raman spectroscopy are in good agreement with the results obtained from transmission electron microscopy (TEM) and photoluminescence spectroscopy (PL) (the PL size distribution is obtained using the model of Delerue *et al.*[16]). This proves the reliability of using Raman spectroscopy with the analytical-PCM for size analysis of Si-NCs. In addition, we also demonstrate the BPM,[11] which is also used for size analysis of semiconductor nanocrystals. **Figure 5** concludes also that the PCM predicts the size of a Si-NC from its size-dependent Raman shift better than the BPM does.
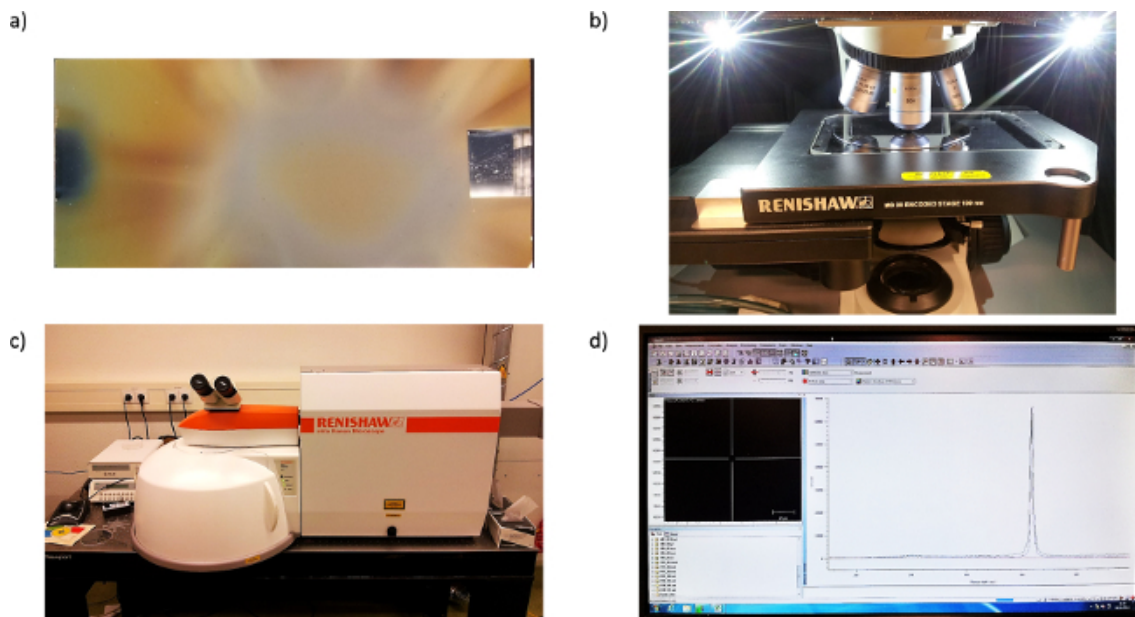
Figure 1. Representation of nanoparticles and the Raman spectrometer. **a**) Si-NCs deposited in an Ar/SiH$_4$ gas mixture on plexiglass substrates using a PECVD tool. Si-NCs are in the form of a powder. The tone differences on the substrate are due to the differences in morphologies and thicknesses of Si-NC powder, which are exposed to different plasma regions during the synthesis[13]. As deposited morphologies of Si-NCs are ready for Raman spectroscopy measurements. The short side of the substrate is 2 cm. **b**) Reference sample, *i.e.*, crystalline Si wafer, measurement in order to observe the Raman peak position of bulk Si. This information will be used as a reference point when determining the relative shift of Si-NCs from their bulk peak position. **c**) Image of the Raman spectrometer used for size determination studies. **d**) The screenshot of the software for performing and recording the data to be analyzed.

a)
$$I(\omega) = \int_{D_{\min}}^{D_{\max}} \Phi(D)\, \mathcal{L}_{Si}(\omega, D)\, dD$$

b)
$$\Phi(D) = e^{\frac{(-\log\frac{D}{D_0})^2}{2\sigma^2}}$$

c)
$$\mathcal{L}_{Si}(\omega, D) \propto \frac{A(D)}{\pi} \frac{\Gamma_{NC}(D)/2}{(\omega - \omega_{NC}(D))^2 + [\Gamma_{NC}(D)/2]^2}$$

d)
$$A(D) = 1.4 \times 10^{-2} \times D^{-3}$$

e)
$$\Gamma_{NC}(D) = \Gamma_{Si} + 60.0 \times D^{-4}$$

f)
$$\omega_{NC}(D) = \omega_{Si} - 34.8 \times D^{-2}$$

Figure 2. Formulas used in the analysis of size distribution of Si-NCs. a) Raman intensity of Si-NCs with size distribution. **b**) The generic size distribution function to determine Si-NC size distribution. **c**) Analytical representation of one-particle PCM for a Si-NC with a size D. **d**) The amplitude, **e**) the full width half maximum, and **f**) the vibration frequency representations of a Si-NC with a size D, which explicitly appear in **c**).
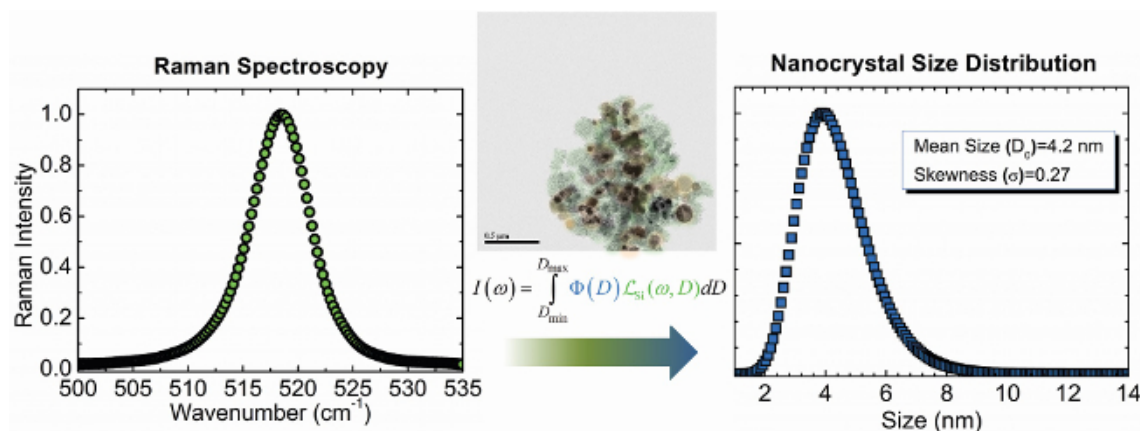

Figure 3. From Raman spectroscopy analysis to nanocrystal size distribution. As-measured data from Raman spectroscopy can be converted to a quantitative size distribution of nanocrystals using the multi-particle analytical-PCM.
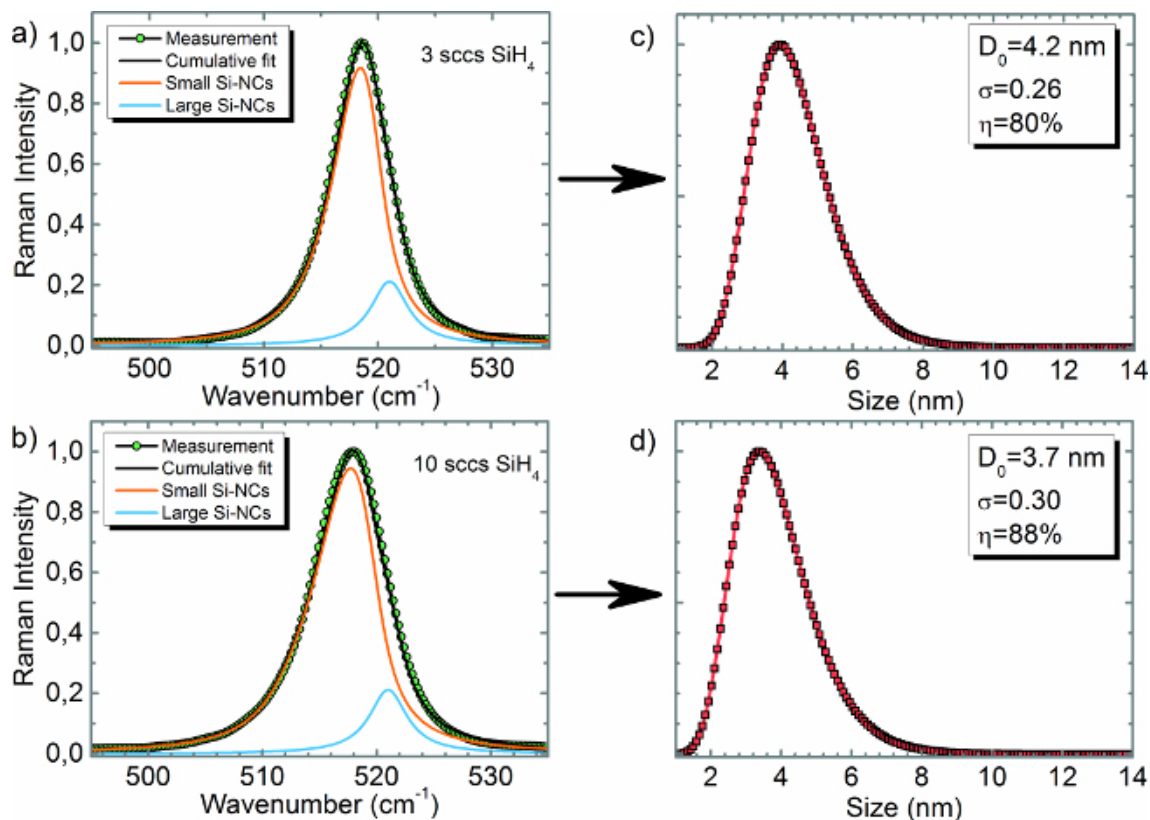
Figure 4. Size and volume fraction analysis of Si-NCs. Raman spectrum of Si-NCs synthesized in a PECVD tool using **a**) 3 sccs and **b**) 10 sccs of SiH_4(silane) gas flow, respectively. **a**) and **b**) demonstrates the deconvolution route for small and large Si-NCs. Deconvolution is done using a Lorentzian peak for bulk-like large Si-NCs and multi-particle analytical-PCM for small Si-NCs. Corresponding size distributions and volume fractions of small Si-NCs for 3 and 10 sccs SiH_4 flow are demonstrated in **c**) and **d**), respectively. The average size of small Si-NCs is 4.2 nm with a skewness of 0.26 for panel **c**) and 3.7 nm with a skewness of 0.30 for panel **d**). The volume fractions are estimated as 80% and 88% for panel **c**) and **d**), respectively.
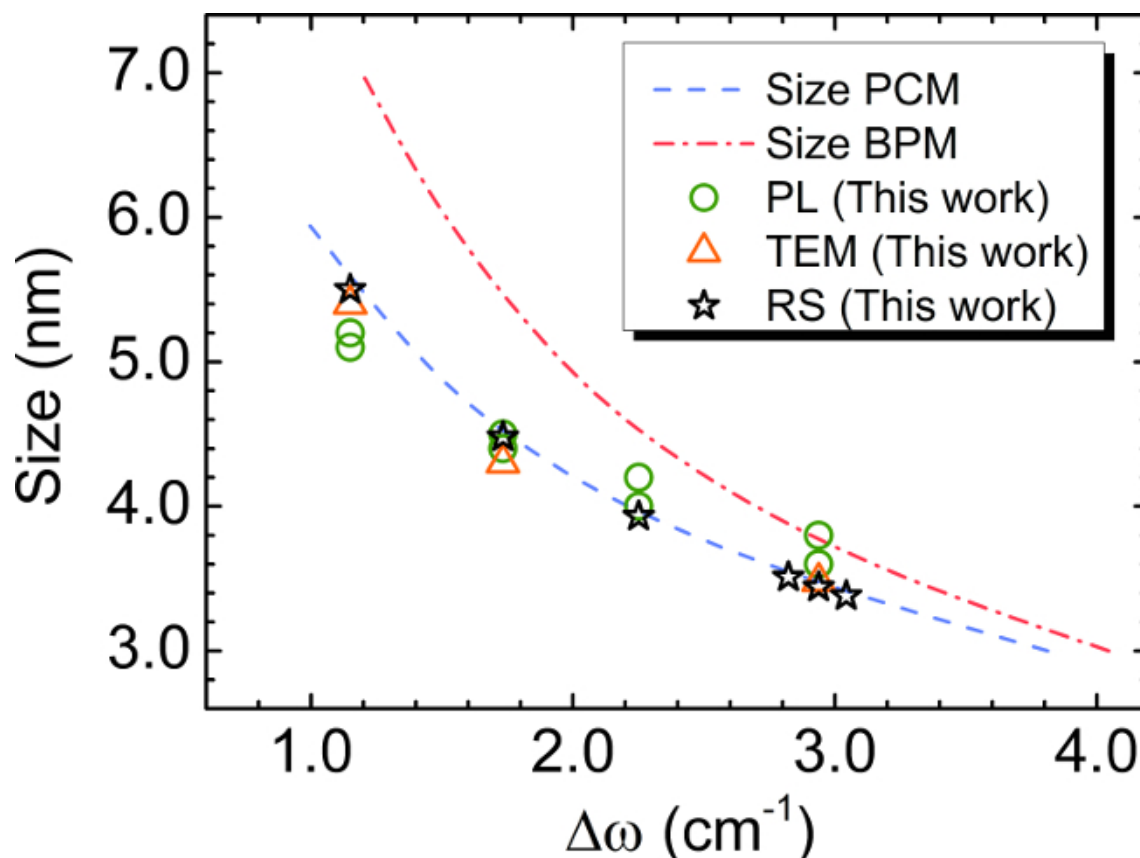
Figure 5. Comparison of size distribution of Si-NCs from various techniques. Size analysis of Si-NCs using various techniques (TEM and PL[16]) and size analysis using Raman spectroscopy resulted in excellent agreement. The results also demonstrate that the PCM leads to a more accurate size determination with respect to the BPM. This figure has been modified from Ref. 12 by permission of American Institute of Physics.

Discussion

First discussion point is the critical steps within the protocol. In order not to have overlapping peaks with the material of interest, it is important to use another type of substrate material as mentioned in step 1.2. For instance, if Si-NCs are of interest, do not use silicon substrate for the Raman measurements. In **Figure 1a**, for instance, Si-NCs were synthesized on plexiglass substrates, which has completely flat signal roughly around the range of interest, *i.e.*, 480-530 cm^{-1}. In addition to measuring a bulk reference signal to estimate the shift of nanocrystal-related peak as mentioned in step 1.4, it is also critical to locate the exact position of the peak of the bulk material, since it can be also shifted depending on the operating and environment conditions of Raman spectroscope. For the case of Si-NCs, the reference sample is a crystalline silicon wafer, which is known to have the transverse optical (TO) mode at 521 cm^{-1}.[12] However, this can be shifted as result of temperature of the operating laser, which is liked with the ambient conditions, and intensity. Therefore, it is important to record a reference data every time before the measurements, and correct them with respect to the known peak positions from the literature. A high laser power can heat up the nanocrystals, and change their sizes, which result in a laser-induced shift in the Raman spectrum. Therefore, it is critical to determine the maximum laser power that can be used safely following the instructions at step 1.5. If inserting the estimated average size and skewness in step 3.4.3 into the fitting function cannot not cover the shape of the measured Raman spectrum, it means that the material analyzed is composed of sub-distributions. Then repeat the steps 3.4.2 and 3.4.3 again to add additional peaks for the fitting. The determination of the integral boundaries (step 3.4.7) for the size distribution is another critical point. The boundaries of the integral in the distribution function represents the smallest and the largest sizes in the nanocrystal size distribution. 1 nm is the smallest stable size for most of the nanocrystal systems.[17] As the amount of size-dependent shift decreases with an increase of the nanocrystal size, set the upper limit of the integration to any size that does not exhibit any shift in the Raman spectrum (step 3.4.8). For instance, Si-NCs with sizes larger than 20 nm does not exhibit any shift in the Raman spectrum, they resemble bulk-like behavior.[10,12] Therefore, for Si-NCs setting the upper boundary of the integral with any size greater than 20 nm will not change the result.

The PCM describes the size-dependent Raman peaks of nanocrystals through a complicated expression. In fact, the PCM depends on the phonon dispersion, the confinement function, and the vibration frequency, which all implicitly depend on the size, *D*. Furthermore, the PCM is for a specific size, and to determine the size distribution, it has to be projected on to a generic distribution function and get integrated over a size range. This procedure is complicated and up to now, experimentalists were using Raman spectroscopy mostly to determine the average size of Si-NCs from the shift of the as-measured Raman peak. On the other hand, the multi-particle analytical-PCM that we have formulized contains the size, *D*, as an explicit parameter and makes it possible to determine not only the average size, but also the complete distribution and it shape in a simple way using Raman spectroscopy.

As already noticed, Raman spectroscopy is able to determine the size distribution of nanocrystals within the confinement limit, which is about 20 nm for Si. Larger sizes cannot be analyzed for their size distribution as they do not exhibit a size-dependent feature in Raman spectrum, *i.e.*,

they have similar peak shapes and positions as bulk crystalline Si. This limitation holds for any type of nanocrystal system that exhibits size-dependent peak-shift in the Raman spectrum. However, the confinement limit can vary depending on the nanocrystal system. For instance, the confinement limit for Ge-NCs is about 15 nm.[18]

A concern during the size analysis of nanocrystals is the shift of the Raman peaks of nanocrystals because of the secondary reasons, which could result in wrong size interpretations using Raman spectroscopy. These secondary reasons are structural modification (grain growth or shape change) of nanocrystals under excessive laser power during Raman measurement, and the stress induced by the matrix, in which nanocrystals are embedded (if any). In order to avoid excessive laser heating, it is advised to start the measurement with the lowest possible laser power and increase it gradually to establish a clear signal. As long as the peak shape and position stays stable independent of the laser power used, it can be considered that the laser power used is in the safe limit.[13] In addition, the limit beyond which, a heating related broadening of the Raman peaks is observed is defined in the literature as the Fano broadening.[12,19] As long as the Fano broadening limit is not reached, nanoparticles are not subject to heating related modifications. If the stress-related peak-shift is present, it is unavoidable, and has to be accounted for before determining the size-dependent peak-shift. The amount of stress can be determined using X-ray diffraction (XRD), where a shift in the diffraction peak position is a measure of stress. The estimated stress can then be accounted in the Raman spectrum with an addition of the stress-dependent peak-shift term.[18] If no stress is observed from XRD, direct analysis of size distribution can be performed from the as-measured Raman spectrum. Since all the nanoparticles have stable structures, as observed previously,[14] the crystallinity is well established, and concerns related with poor crystalline structures are ruled out for the Raman analysis.

The multi-particle analytical-PCM demonstrated in **Figure 2a** is flexible in terms of the distribution function and the confinement function used. For instance, any type of generic distribution function can be replaced with lognormal distribution function, *i.e.* it could be a lognormal, normal, or a logistic function, without affecting the phonon confinement function. In addition, the analytical-PCM demonstrated in **Figure 2c** can be re-defined depending on the type of the material to be used. Some nanocrystal systems that exhibit size-dependent Raman peak-shifts (so that their size distributions can also be determined using Raman spectroscopy) are Ge-NCs,[20] SnO$_2$-NCs,[21] TiO$_2$-NCs,[22] and diamond-NCs.[23]

Disclosures

The authors have nothing to disclose.

Acknowledgements

References

1. Goller, B., Polisski, S., Wiggers, H., Kovalev, D. Freestanding spherical silicon nanocrystals: A model system for studying confined excitons. *Appl Phys Lett.* **97**, (4), 041110 (2010).
2. Luo, J. -W., Franceschetti, A., Zunger, A. Carrier multiplication in semiconductor nanocrystals: theoretical screening of candidate materials based on band-structure effects. *Nano lett.* **8**, (10), 3174-3181 (2008).
3. Govoni, M., Marri, I., Ossicini, S. Carrier multiplication between interacting nanocrystals for fostering silicon-based photovoltaics. *Nat. Photonics.* **6**, (September), 672-679 (2012).
4. De Boer, W. D. A. M., Gregorkiewicz, T., *et al.* Step-like enhancement of luminescence quantum yield of silicon nanocrystals. *Nat nanotechnol.* **6**, (11), 1-4 (2011).
5. Sun, L., Choi, J. J., *et al.* Bright infrared quantum-dot light-emitting diodes through inter-dot spacing control. *Nat nanotechnol.* **7**, (6), 369-373 (2012).
6. Maier-Flaig, F., Rinck, J., *et al.* Multicolor Silicon Light-Emitting Diodes (SiLEDs). *Nano lett.* **13**, (2), 1-6 (2013).
7. Patterson, A. L. The Scherrer Formula for X-Ray Particle Size Determination. *Phys Rev.* **56**, (10), 978-982 (1939).
8. Borchert, H., Shevchenko, E. V., *et al.* Determination of nanocrystal sizes: a comparison of TEM, SAXS, and XRD studies of highly monodisperse CoPt3 particles. *Langmuir.* **21**, (5), 1931-1936 (2005).
9. Heitmann, J., Müller, F., Zacharias, M., Gösele, U. *Silicon Nanocrystals: Size Matters. Adv Mat.* **17**, (7), 795-803 (2005).
10. Faraci, G., Gibilisco, S., Russo, P., Pennisi, A., La Rosa, S. Modified Raman confinement model for Si nanocrystals. *Phys Rev B.* **73**, (3), 1-4 (2006).
11. Zi, J., Büscher, H., Falter, C., Ludwig, W., Zhang, K., Xie, X. Raman shifts in Si nanocrystals. *Applied Physics Letters.* **69**, (2), 200 (1996).
12. Doğan, İ, van de Sanden, M. C. M. Direct characterization of nanocrystal size distribution using Raman spectroscopy. *J. Appl. Phys.* **114**, 134310 (2013).
13. Doğan, I., Kramer, N. J., *et al.* Ultrahigh throughput plasma processing of free standing silicon nanocrystals with lognormal size distribution. *J. Appl. Phys.* **113**, 134306 (2013).
14. Doğan, İ, Weeks, S. L., Agarwal, S., van de Sanden, M. C. M. Nucleation of silicon nanocrystals in a remote plasma without subsequent coagulation. *J Appl Phys.* **115**, (24), 244301 (2014).
15. Doğan, İ, Westermann, R. H. J., van de Sanden, M. C. M. Improved size distribution control of silicon nanocrystals in a spatially confined remote plasma. *Plasma Sources Sci. Technol.* **24**, 015030 (2015).
16. Delerue, C., Allan, G., Lannoo, M. Theoretical aspects of the luminescence of porous silicon. *Phys Rev B.* **48**, (15), 11024 (1993).
17. Boufendi, L., Jouanny, M. C., Kovacevic, E., Berndt, J., Mikikian, M. Dusty plasma for nanotechnology. *J. Phys. D: Appl. Phys.* **44**, (17), 174035 (2011).
18. Wellner, A., Paillard, V., *et al.* Stress measurements of germanium nanocrystals embedded in silicon oxide. *J Appl Phys.* **94**, (2003), 5639-5642 (2003).

19. Faraci, G., Gibilisco, S., Pennisi, A. R. Quantum confinement and thermal effects on the Raman spectra of Si nanocrystals. *Phys. Rev. B.* **80**, (19), 1-4 (2009).

20. Roodenko, K., Goldthorpe, I. A., McIntyre, P. C., Chabal, Y. J. Modified phonon confinement model for Raman spectroscopy of nanostructured materials. *Phys. Rev. B.* **82**, (11), 115210 (2010).

21. Diéguez, A., Romano-Rodríguez, A., Vilà, A., Morante, J. R. The complete Raman spectrum of nanometric SnO[sub 2] particles. *J. Appl. Phys.* **90**, (3), 1550 (2001).

22. Bersani, D., Lottici, P. P., Ding, X. -Z. Phonon confinement effects in the Raman scattering by TiO[sub 2] nanocrystals. *Appl. Phys. Lett.* **72**, (1), 73 (1998).

23. Lipp, M., Baonza, V. G., Evans, W. J., Lorenzana, H. E. Nanocrystalline diamond: Effect of confinement, pressure, and heating on phonon modes. *Phys. Rev. B.* **56**, (10), 5978-5984 (1997).